Electronic Supplementary Material (ESI) for Journal of Materials Chemistry A.
This journal is © The Royal Society of Chemistry 2016

ESI:

Facile one-pot solvothermal preparation of Mo-doped Bi_2WO_6 biscuit-like microstructures for visible-light-driven photocatalytic water oxidation

Atangana Etogo,[a] Ren Liu,[a] Jiabin Ren,[a] Liwen Qi,[a] Changcheng Zheng,[b] Jiqiang Ning,[c] Yijun Zhong,[a] and Yong Hu[a,d]*

[a]*Institute of Physical Chemistry, Zhejiang Normal University, Jinhua, 321004, P. R. China. E-mail：*yonghu@zjnu.edu.cn

[b]*Mathematics and Physics Centre, Department of Mathematical Sciences, Xi'an Jiaotong-Liverpool University, Suzhou 215123, P. R. China*

[c]*Vacuum Interconnected Nanotech Workstation, Suzhou Institute of Nano-Tech and Nano-Bionics, Chinese Academy of Sciences, Suzhou 215123, P. R. China*

[d]*State Key Lab of Silicon Materials, College of Materials Science and Engineering, Zhejiang University, Hangzhou, 310027, P. R. China*

The quantum efficiency (QE) for O_2 production under visible-light illumination was determined using the following equation:

$$\mathrm{QE}[\%]=\frac{\text{the number of evolved } \mathrm{O_2} \text{ molecules} \times 4}{\text{the number of incident photons}} \times 100\%$$

The quantum efficiency QE could also be was evaluated by the equation:

$$\mathrm{QE} = 4n_{O2}/n_p \times 100\%$$

The mole of photons absorbed by the photosensitizer (n_p) was determinated by the following equation:

$$n_p = Pt\lambda \,/\, N_A hc$$

Where n_p represents moles of photons absorbed by the photosensitizer, P(W) is the absorbed power of the light, t is the irradiation time (21600 s). λ is the irradiation wavelength number (420, 450 and 500), N_A is the Avogadro constant (6.022×10^{23} mol^{-1}), h is the Planck constant (6.63×10^{-34} J·s) and c is the speed of the light (3×10^{8}m.s^{-1}).

The measured light power is 151.9, 174.7 and 212.5mW at 420, 450 and 500nm, respectively. The evolved O_2 (n_{O2}) were determined to be 8.83×10^{-5} mol and 3.66×10^{-5} mol for $Bi_2Mo_{0.21}W_{0.79}O_6$ and Bi_2WO_6 by GC after 6h light irradiation, respectively. For $Bi_2Mo_{0.21}W_{0.79}O_6$ sample, the apparent QE values were 3.1 %, 2.5%, and 1.8% at 420, 450 and 500 nm, respectively, representing that the value decreased gradually as the incident light wavelength increased. However, the apparent QE at 420 nm of pristine Bi_2WO_6 was measured to be 1.2%, indicating almost 3 fold enhancement after Mo doping.

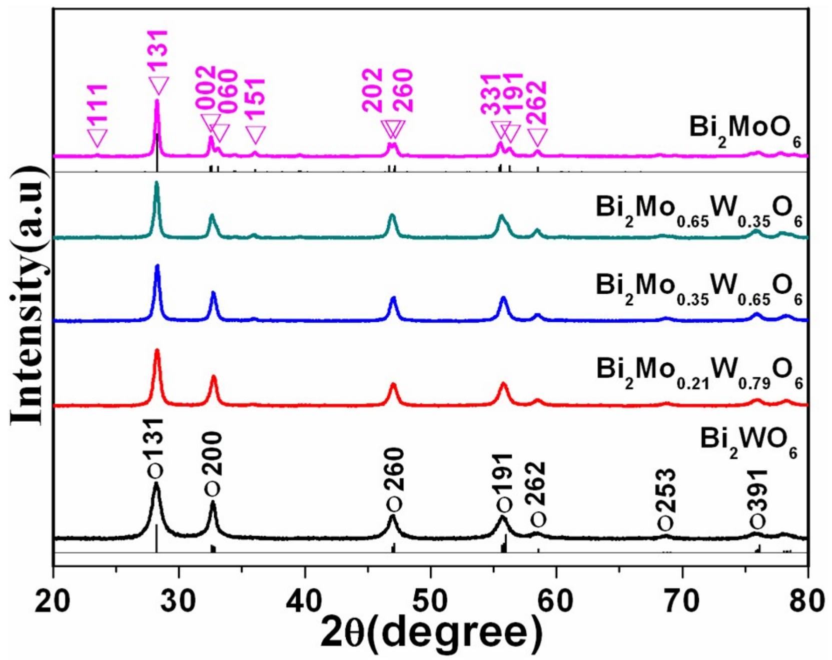

Fig. S1 XRD patterns of as-prepared Bi_2WO_6, Bi_2MoO_6 and Mo-doped Bi_2WO_6 samples.

photocatalysts	a (Å)	b (Å)	c (Å)
B_2iWO_6	5.610	5.571	16.819
$Bi_2Mo_{0.25}W_{0.75}O_6$	5.630	5.588	16.765
$Bi_2Mo_{0.5}W_{0.5}O_6$	5.654	5.608	16.754
$Bi_2Mo_{0.75}W_{0.25}O_6$	5.650	5.628	16.615

Table S1 Lattice parameters as a function of Mo^{6+} dopant concentration.

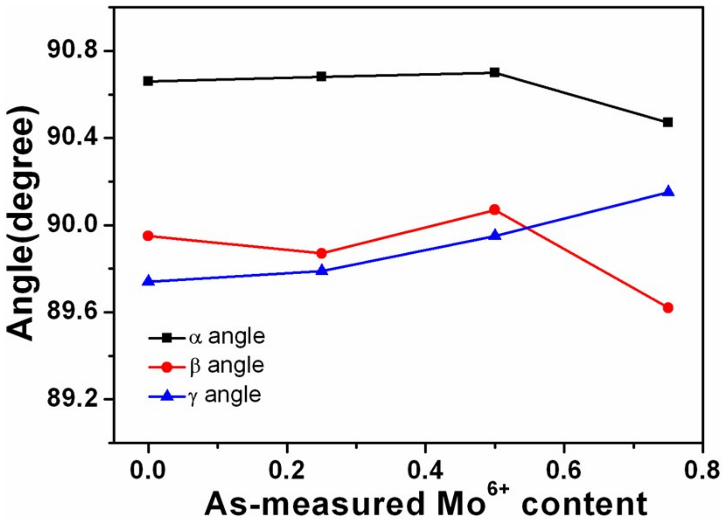

Fig S2 α, β and γ angles as a function of Mo^{6+} dopant concentration.

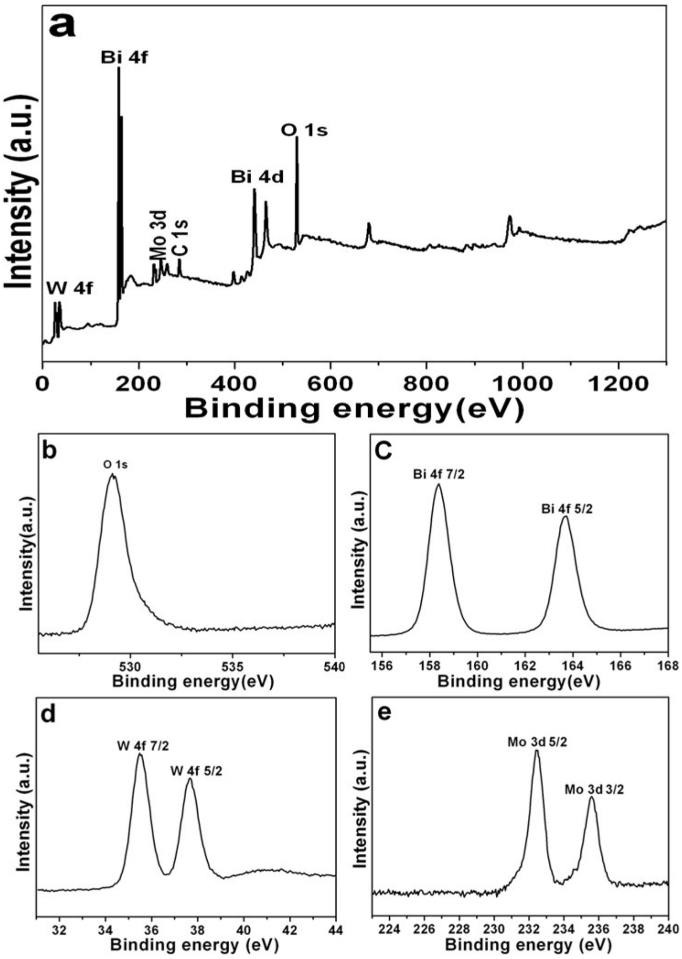

Fig. S3 XPS spectra of $Bi_2Mo_{0.21}W_{0.79}O_6$ PBMs: (a) Survey spectrum, (b) O 1s, (c) Bi 4f , (d) W4f and (e) Mo 3d.

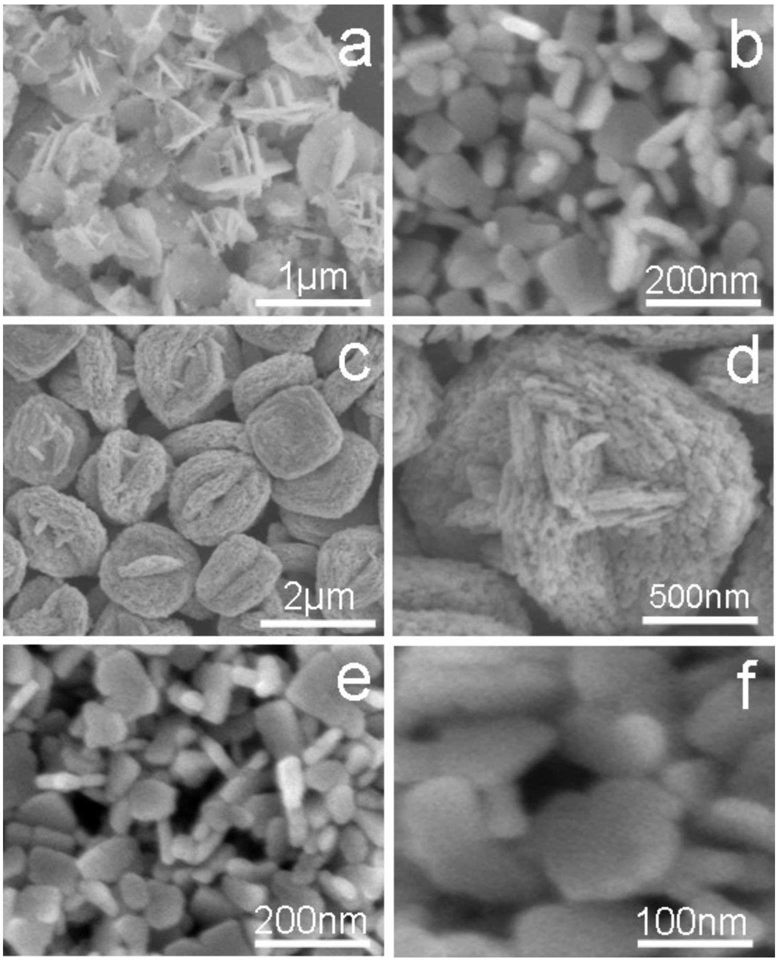

Fig. S4 SEM images of the as-prepared (a) Bi_2WO_6, (b) Bi_2MoO_6 nanostructures, (c, d) $Bi_2Mo_{0.35}W_{0.65}O_6$, (e, f) $Bi_2Mo_{0.65}W_{0.35}O_6$.

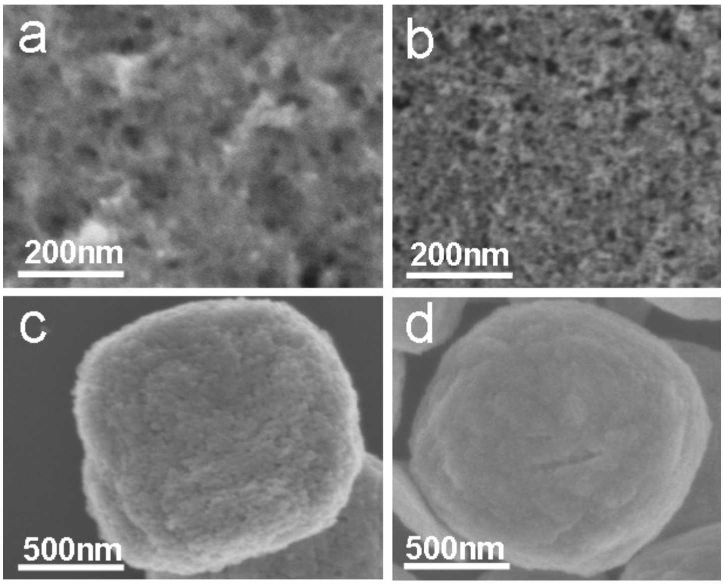

Fig. S5 SEM images of the products obtained (a) room temperature under continuous stirring after 20min, (b) 180 °C for 1.5h, (c) 180 °C for 5h and (d) 180 °C for 10h.

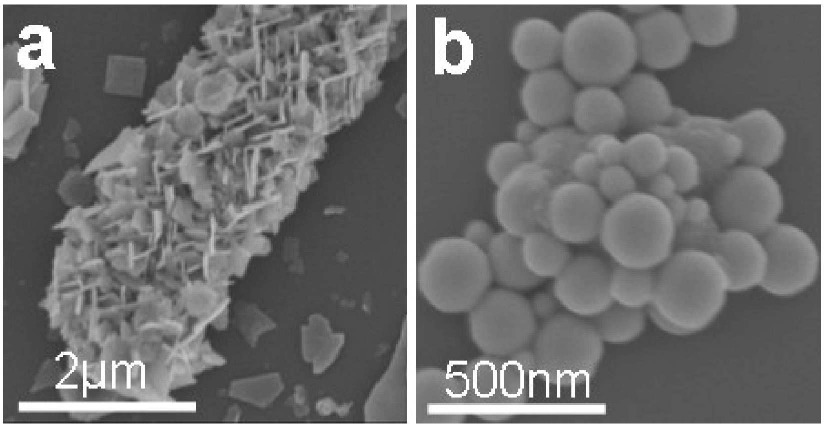

Fig. S6 SEM images of the products obtained at 180°C (a) using water as solvent, (b) using ethylene glycol as solvent.

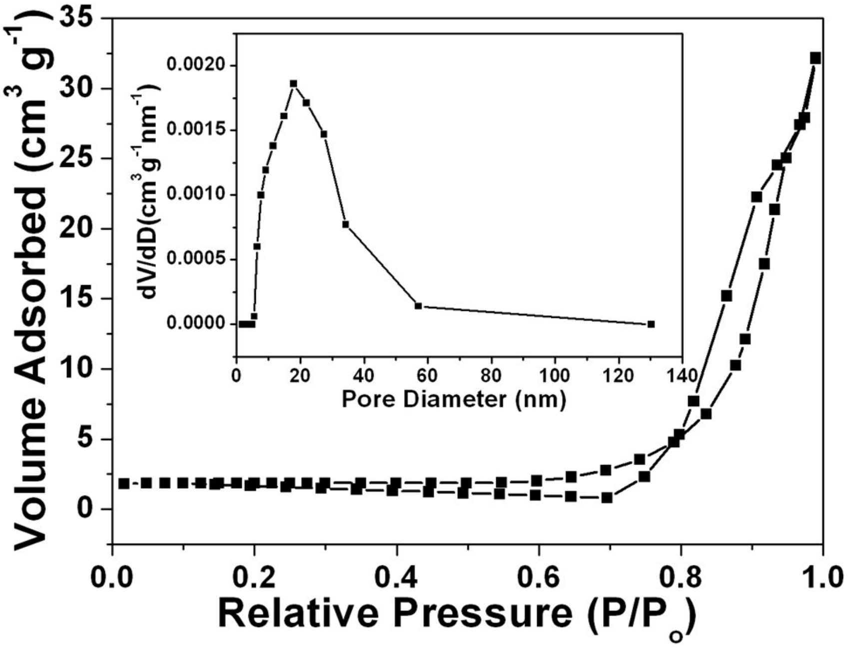

Fig. S7 N_2 adsorption–desorption isotherm and pore-size distribution curve of the as-obtained $Bi_2Mo_{0.21}W_{0.79}O_6$ PBMs.

.

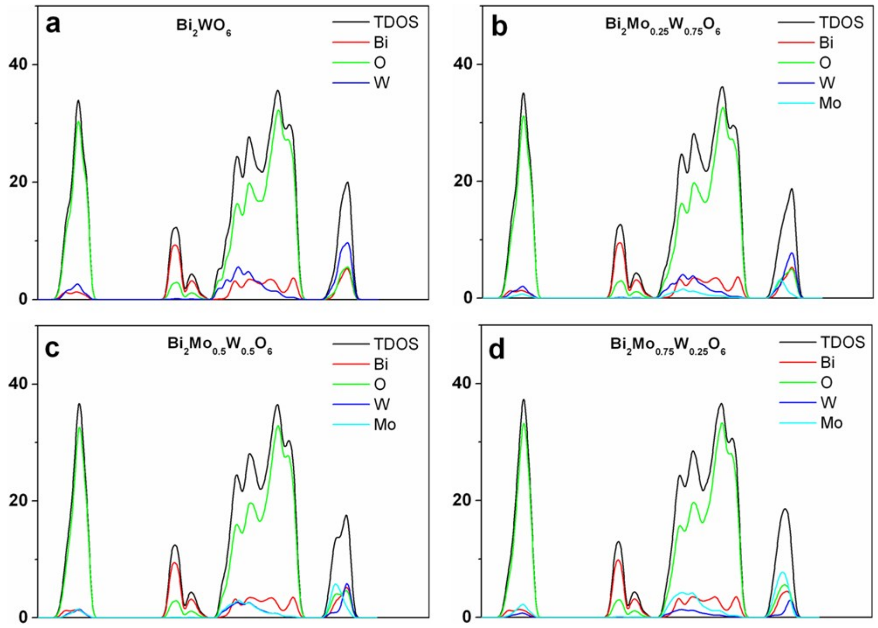

Fig. S8 Partial density of states (PDOS) of (a) Bi_2WO_6,(b) $Bi_2Mo_{0.25}W_{0.75}O_6$,(c) $Bi_2Mo_{0.5}W_{0.5}O_6$ and (d) $Bi_2Mo_{0.75}W_{0.25}O_6$ samples.

To rule out the heat driven O_2 evolution, a series of experiments were carried out at 40°C and 60°C by a precision bath circulator (Tianheng, THD-05) without visible-light irradiation, respectively. In a typical reaction, 100mg of $Bi_2Mo_{0.21}W_{0.79}O_6$ PBMs in 100 mL aqueous solution containing 0.1 M NaOH, 0.02 M $Na_2S_2O_8$ were added to the reactor under magnetic vigorous stirring to ensure the mixture suspense. The suspension was purged with argon for at least 90 min to drive off the air inside. Analysis of the evolved O_2 was performed using an online gas chromatograph (Agilent Technologies GC-7890B, TCD, Ar carrier gas). As it can be seen in **Fig. S10** (see ESI†), no O_2 was produced after 6 h at 40°C or 60°C. This result demonstrates that the O_2 can only be generated under visible-light irradiation. In our experiment, the photocatalytic water oxidation was carried out at 20°C±2 C by a continuous water circulator. The relevant modifications were mentioned in the manuscript

.

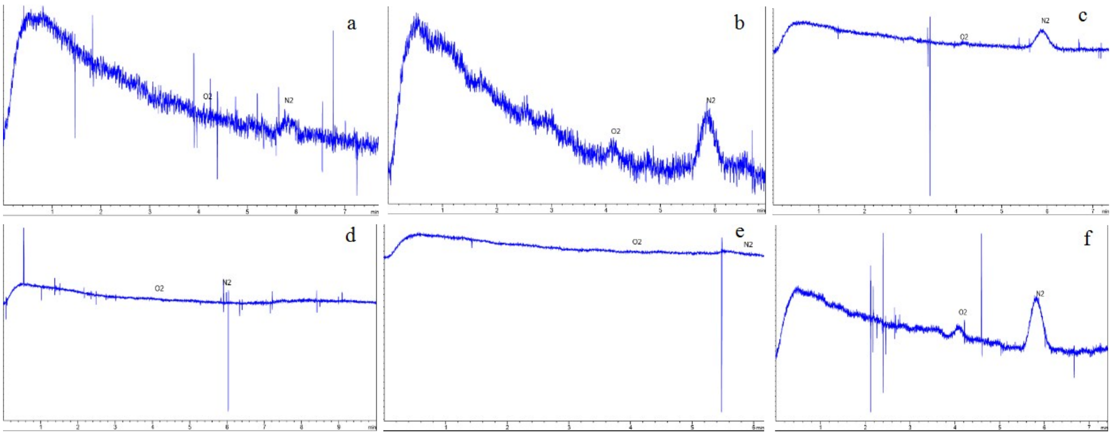

Fig. S9. O_2 evolution reference tests with $Na_2S_2O_8/Co_3O_4$-$Bi_2Mo_{0.21}W_{0.79}O_6$ PBMs at 40°C after (a) 1h , (b) 3h, (c) 6h and at 60°C after (d) 1h, (e) 3h and (f) 6h.

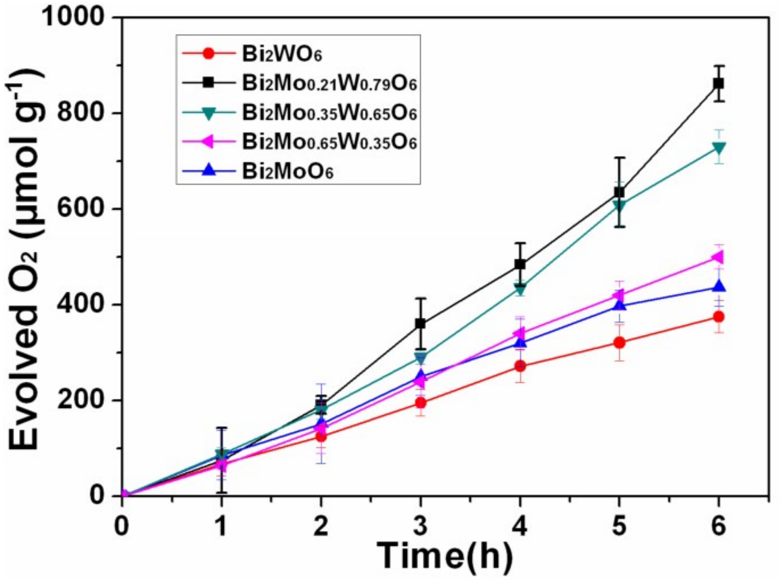

Fig. S10 Repeat photocatalytic oxygen evolution and standard deviations from water splitting over Bi_2WO_6, $Bi_2Mo_{0.21}W_{0.79}O_6$, $Bi_2Mo_{0.35}W_{0.65}O_6$, $Bi_2Mo_{0.65}W_{0.35}O_6$ and Bi_2MoO_6 samples (and samples with 5%wt deposited Co_3O_4) under visible-light irradiation. Reaction conditions: 0.1 g photocatalyst, 100 mL 0.1 M NaOH and 0.02 M $Na_2S_2O_8$ aqueous solution.

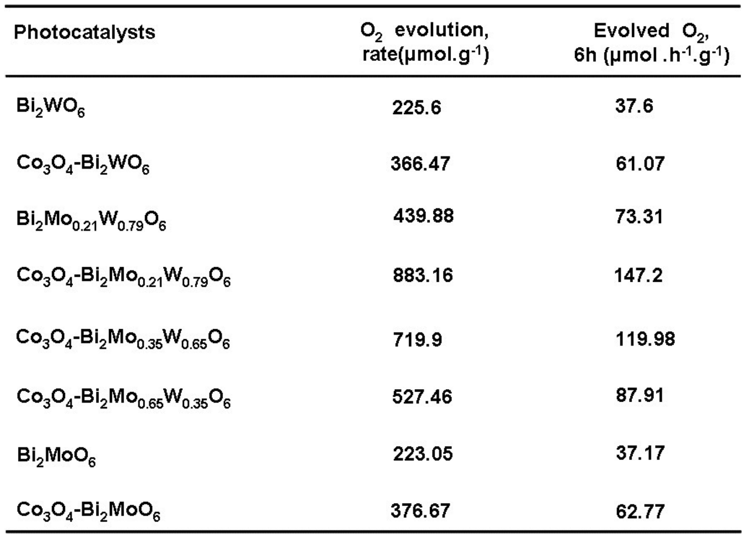

Photocatalysts	O_2 evolution, rate(μmol.g^{-1})	Evolved O_2, 6h (μmol .h^{-1}.g^{-1})
Bi_2WO_6	225.6	37.6
Co_3O_4-Bi_2WO_6	366.47	61.07
$Bi_2Mo_{0.21}W_{0.79}O_6$	439.88	73.31
Co_3O_4-$Bi_2Mo_{0.21}W_{0.79}O_6$	883.16	147.2
Co_3O_4-$Bi_2Mo_{0.35}W_{0.65}O_6$	719.9	119.98
Co_3O_4-$Bi_2Mo_{0.65}W_{0.35}O_6$	527.46	87.91
Bi_2MoO_6	223.05	37.17
Co_3O_4-Bi_2MoO_6	376.67	62.77

Table S2 Photocatalytic oxygen evolution rates for all the samples

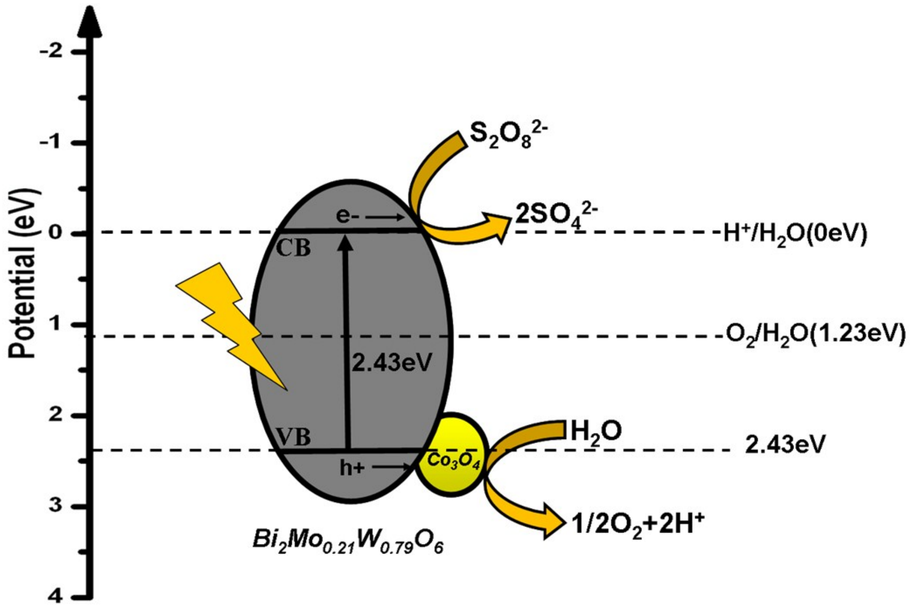

Fig. S11 Schematic diagram showing possible water oxidation reaction catalyzed by the $Co_3O_4/Bi_2Mo_{0.21}W_{0.79}O_6$ PBMs samples under UV-visible light irradiation ($\lambda > 420$ nm).

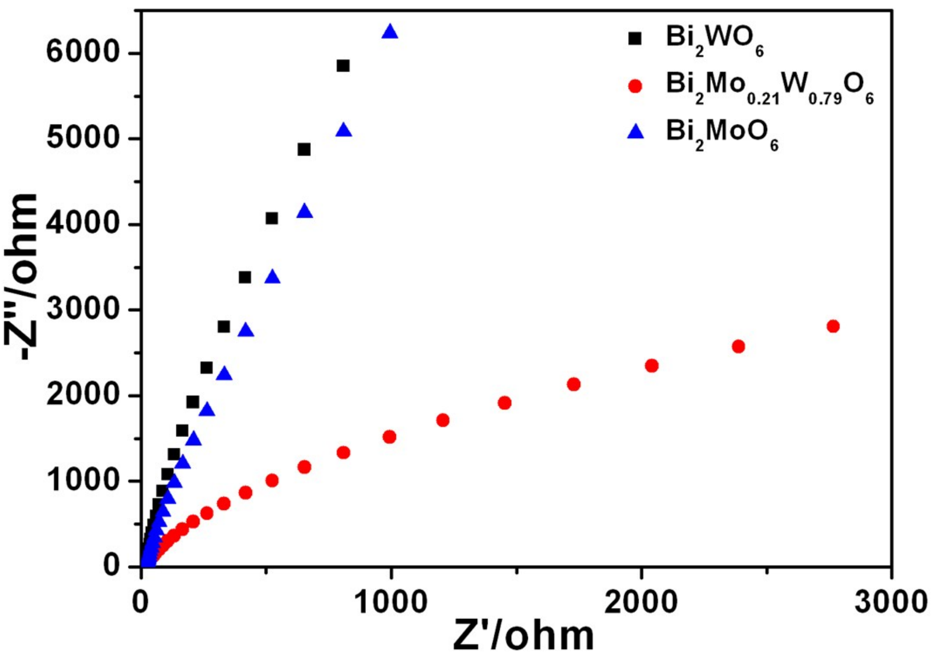

Fig. S12 lectrochemical impedance spectra of the as-prepared Bi_2WO_6, Bi_2MoO_6 and $Bi_2Mo_{0.21}W_{0.79}O_6$ PBMs.

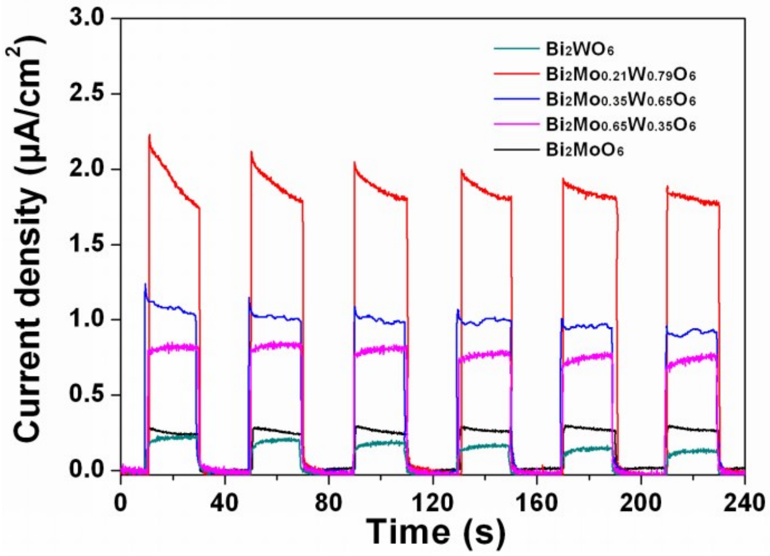

Fig. S13 Photocurrent response of the different samples under visible-light illumination.